

Electric field selectivity and multiplexing of volume holograms in LiNbO₃

V.M. Petrov¹, C. Denz¹, A.V. Shamray², M.P. Petrov², T. Tschudi¹

¹ Institute of Applied Physics, Darmstadt University of Technology, Hochschulstrasse 6, 64293 Darmstadt, Germany
(Fax: +49-6151/163-122, E-mail: victor.petrov@physik.tu-darmstadt.de)

² A. F. Ioffe Physical Technical Institute, Polytechnicheskaiya st., 26, St. Petersburg 194021, Russia
(Fax: +7-812/247-1017, E-mail: mpetr@pop.ioffe.rssi.ru)

Received: 5 January 2000/Revised version: 18 February 2000/Published online: 27 April 2000 – © Springer-Verlag 2000

Abstract. Theoretical and experimental investigations of electric field multiplexing and selectivity of reflection volume holograms in LiNbO₃ are reported. Recording of at least five holograms is demonstrated. Equivalent spectral selectivity $\Delta\lambda \approx 4.5$ pm for the case of three electrically tunable holograms and $\Delta\lambda \approx 9$ pm for the case of five electrically tunable holograms are estimated.

PACS: 42.40; 42.70; 72.40

Diffraction from volume holograms obeys the Bragg condition. As a result the hologram exhibits strong angular or spectral selectivities [1]. In the case when the volume hologram is recorded in an electro-optic crystal, the Bragg condition can be controlled by applying an external electric field due to variations of the average refractive index of the material via the electro-optic effect [2–7]. This results in a strong electric field selectivity (EFS). The high selectivity provides the possibility to record and retrieve many holograms in the same volume of a material, i.e. provides multiplexing of volume holograms. Photorefractive crystals represent a well-suited class of materials for electric field multiplexing (EFM) because the electro-optic effect is their inherent property. Although the first demonstrations of EFM were made many years ago [2], the interest to EFS and EFM increased sharply only in the last few years [3–7] because electrically controlled volume holograms can be used as tunable spectral filters with a very high (of the order 10^4 – 10^6) quality factor. Such filters are an appropriate component for fiber wavelength division multiplexing systems, for electrically controlled sources of coherent radiation, and many other applications.

Although the principles of EFS and EFM are described in the above-mentioned papers, there are up to now only a very few experimental data on this subject. Consequently, a better understanding of EFS and EFM is needed in order to allow the realization of competitive devices.

In this paper we describe the optimal experimental configuration for EFS in LiNbO₃, present a comparison between

theoretical and experimental data for EFS in dependence on the applied electric field, the thickness of the hologram, and the exposition during recording. An excellent agreement between theory and experiment was found for EFS in the case of recording a single hologram. Then we experimentally demonstrate the potential of EFS and EFM when recording at least five holograms, and discuss the origin of crosstalk.

It was shown that an electrically controlled hologram can operate as a tunable spectral filter with selectivity $\Delta\lambda/\lambda \approx 10^{-5}$.

1 Theory

The Bragg condition for a volume hologram has the form:

$$\frac{1}{\Lambda} = \frac{2n_{av}}{\lambda} \sin \Theta_B, \quad (1)$$

where Λ is the grating spacing, λ is the light wavelength in the vacuum, n_{av} is the refractive index (the periodical modulation of the refractive index due to recording of the hologram is assumed to be much less than n_{av}) and Θ_B is the Bragg angle in the media. The violation of the Bragg condition by changing λ or Θ during readout of the hologram leads to decreasing of the diffraction efficiency. Acceptable changes of λ or Θ are characterized by spectral and angular selectivity, which depend mostly on the thickness of the hologram. Because a variation of the refractive index will also lead to a decrease in the diffraction efficiency, the case of refractive index changing under influence of external electric field will lead to the same behavior in EFS. For a reflection hologram (at $\Theta_B \approx 90^\circ$) with a hologram thickness T , it can be shown [2, 4–6] that this EFS can be estimated as:

$$\frac{\Delta n_{av}}{n_{av}} \approx \frac{\Delta\lambda}{\lambda} \approx \frac{\Lambda}{T}, \quad (2)$$

where Δn_{av} is the variation of the average refractive index due to electric field. We ignore here the piezoelectric effect.

The relationship (2) is useful for the estimation of the refractive index variation necessary to change the diffraction efficiency from its maximum value to its first zero. However, to obtain a theoretical expression for the dependence of the diffraction efficiency on E_0 , which causes Δn_{av} , we have to consider a specific geometry including the orientation of the crystal, the direction of the applied electric field E_0 , the direction of light propagation, and the orientation of the light polarization during hologram reconstruction. Our analysis described in [5–7] shows that we are able to meet the conflicting situation between the requirement of high diffraction efficiency and high sensitivity of Δn_{av} on applied field E_0 . The condition which is closest to the optimal one for LiNbO₃ and for the extraordinary beams is found when the wave vector \mathbf{K}_g of the grating is oriented in the range of 30°–50° relative to the C axis of the crystal. Then, the transverse electro-optic effect must be used and the electric field must be oriented perpendicular to \mathbf{K}_g . In this case diffraction efficiency is described by Kogelnik's theory [8] and has a form:

$$\eta = \frac{1}{\left(\frac{\xi}{\nu}\right)^2 + \left[1 - \left(\frac{\xi}{\nu}\right)^2\right] \operatorname{cth}^2\left(\sqrt{\nu^2 - \xi^2}\right)}. \quad (3)$$

Here [7]:

$$\nu = \frac{\pi n_1 T}{\lambda \sin \Theta_B}$$

is the parameter that determines the diffraction efficiency in the case when the Bragg condition is matched ($\xi = 0$),

$$\xi = \frac{2\pi n_{av}}{\lambda} T \left(\frac{\Delta n_{av}}{n_{av}} \right) \sin \Theta_B$$

is the detuning parameter, and

$$n_1 = \frac{\delta D}{|K_g|n_e} r_{sc}^e, \quad \Delta n_{av} = \frac{1}{2} n_e^3 r_{eff}^e E_0,$$

where δD is the amplitude of space-charge grating field. The electro-optic coefficients are signed by

$$r_{sc}^e = \frac{1}{\varepsilon_{33}} (r_{13} n_0^4 \cos^2 \alpha + r_{33} n_e^4 \sin^2 \alpha) - \frac{1}{\varepsilon_{11}} (r_{22} n_0^4 \sin \alpha \cos \alpha + r_{51} n_e^2 n_0^2 \sin^2 \alpha),$$

$$r_{eff}^e = \left(\frac{n_0}{\sqrt{(n_e \cos \alpha)^2 + (n_0 \sin \alpha)^2}} \right)^3 (r_{13} \sin \alpha + r_{33} \sin \alpha \tan^2 \alpha + 2r_{51} \sin \alpha - r_{22} \cos \alpha) \cos^2 \alpha,$$

with n_0 and n_e being the refractive index for ordinary and extraordinary beams, $\varepsilon_{33}, \varepsilon_{11}$ the dielectric permittivities, $r_{13}, r_{33}, r_{51}, r_{22}$ the electro-optic coefficients, and $n_{av} = n_e$. From the expression for r_{eff}^e and r_{sc}^e one can see that the optimal orientation for these parameters do not coincide and selection of the proper orientation depends on a desirable criteria. In our case we oriented the crystal with $\alpha = 30^\circ$, an orientation that is close to the optimal.

The theoretical calculations are presented in Fig. 1a for η in dependence of the external electric field for the following

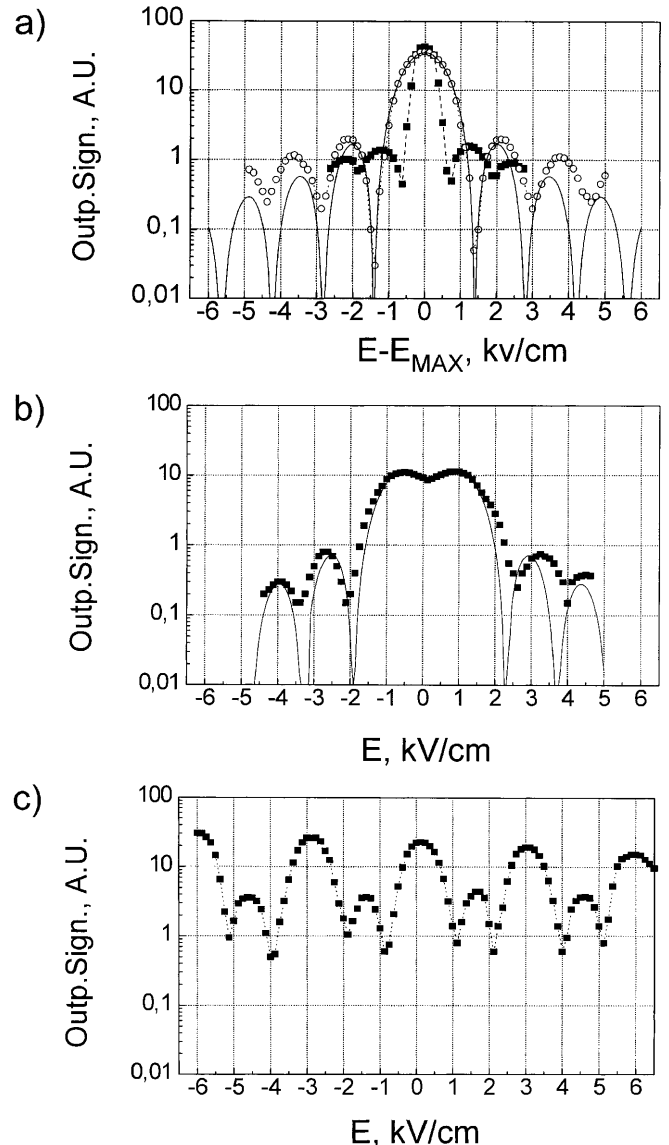


Fig. 1. **a** Diffraction efficiency of one recorded hologram versus the electric field $E - E_{MAX}$. Experiment: \circ – $T = 7$ mm, \blacksquare – $T = 14$ mm. The solid curve is the theoretical dependence using formulae (3), $T = 7$ mm. **b** Diffraction efficiency of two recorded holograms versus the external electric field E . The holograms were recorded at the Rayleigh's criterion. The solid curve is the theoretical dependence based on (3). **c** Diffraction efficiency of five recorded holograms versus the external electric field E . The crystal thickness is 7 mm

parameters: $n_0 = 2.329$, $n_e = 2.232$, $r_{13} = 8.6 \times 10^{-12}$ m/V, $r_{33} = 30.8 \times 10^{-12}$ m/V, $r_{51} = 28.0 \times 10^{-12}$ m/V, $r_{22} = 4.3 \times 10^{-12}$ m/V, $\eta = 5\%$.

2 Experiment

2.1 Experimental setup

The experimental setup for the investigations of EFM is shown in Fig. 2. A Nd:YAG cw laser (1) with intracavity frequency doubling and with $I \approx 100$ mW output power at $\lambda = 523$ nm and extraordinary polarization was used. After

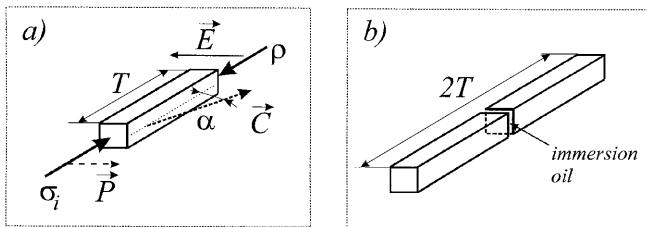
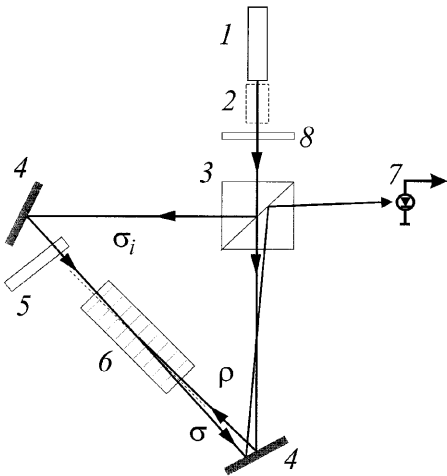


Fig. 2a,b. Experimental setup. 1 – Nd:YAG cw ADLAS laser, $\lambda = 532$ nm, 2 – beam expander, 3 – beamsplitter, 4 – mirrors, 5 – shutter, 6 – crystal, 7 – photodiode, 8 – gray filter. **Insert a** Orientation of the LiNbO_3 crystal. ϱ , σ_i are the recording beams, α is the angle between the optical axis C and the direction of the light propagation, P is the orientation of the wave polarization, E is the external electric field, T is the thickness of the crystal. **Insert b** The double-crystal geometry

passing through the beam expander (2), which consists of a microlens, a pinhole, and a collimating lens, the plane wave was splitted into two beams: σ_i and ϱ . The sample of the LiNbO_3 crystal (6) was illuminated from the opposite sides by recording beams σ_i and ϱ . In this case the Bragg angle Θ_B was approximately $89^\circ 30'$. Using a set of gray filters (8), we could vary the power of the recording beams. After recording of a hologram, the beam σ_i was blocked by shutter (5) and the reconstructed beam σ was detected by a photodiode (7). By applying different electric fields E to the pair of electrodes (not shown in the figure) the dependence of the diffraction efficiency on the electric field E was measured.

Two Fe^{2+} doped single crystals of LiNbO_3 were used. The concentration of Fe^{2+} was less than 0.05 mol %. The orientation of the crystals is shown in Fig. 2a. The pair of electrodes was deposited on the right and left surfaces, the distance between electrodes was 2.5 mm.

Our investigations of EFS and EFM were performed with two different samples of recording media. The first one was a usual sample ($T = 7$ mm) of single crystal for holographic recording. The second was a sample which consists of two separate crystals: one crystal was arranged behind the another (Fig. 2b). In this case, we created an artificial sample with double thickness ($T \approx 14$ mm). In order to reduce cross-reflections from internal sides of crystals, the air gap between the two crystals was filled with immersion oil with $n \approx 1.9$.

2.2 Experimental results

Figure 1a shows the diffraction efficiency of a single recorded hologram as a function of the electric field for two different thicknesses of the hologram $T = 7$ mm and $T = 14$ mm. During our experiments, different holograms were recorded under different experimental conditions. Consequently, the diffraction efficiency reached its maximum at the different electric fields E_{MAX} . That is why using the scale $E - E_{\text{MAX}}$ we can compare data of two different experiments. From this data we are able to estimate EFS. The diffraction efficiency reaches its first minimum approximately at 1.5 kV/cm at $T = 7$ mm and 0.75 kV/cm at $T = 14$ mm. It is obvious that the doubled thickness of a hologram provides twice as much EFS.

Figure 1b shows the diffraction efficiency of two recorded holograms versus the electric field E . The two holograms were recorded with a separation according to the Rayleigh's criterion: the second hologram was recorded at a value of the electric field, at which the first hologram reaches its first minimum. The decrease of the diffraction efficiency between two holograms is approximately 20% which is quite close to the theoretical limit.

Figure 3 shows two dependences: the first one is the ratio between the central maximum of the diffraction efficiency and its first lateral maximum, and the second dependence is the maximum value of diffraction efficiency versus the exposition of recording. From these data the optimal regime of recording was chosen. The exposition was of the order 6.9 J/cm^2 .

Figure 1c shows the diffraction efficiency of five recorded holograms versus the electric field E . The holograms were recorded with a separation of 3 kV/cm . This step is equal to the doubled step at Rayleigh's criterion. Additional (small) maxima appear between major maxima. They appear at the same electric field, at which we have the minimum in diffraction efficiency for the case of only one hologram (see Fig. 1a). For qualitative estimations we can use the ratio between low and high maxima as a criterion of a crosstalk between holograms at a certain separation value of the electric field.

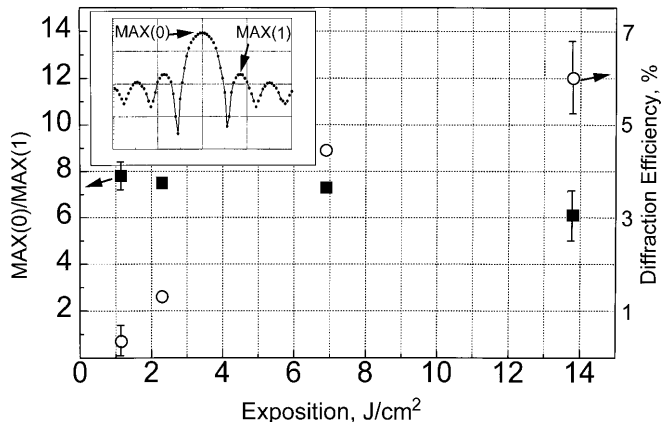


Fig. 3. The ratio between the central maximum – $\text{MAX}(0)$ and the first lateral maximum – $\text{MAX}(1)$ (left scale, ■) and the maximum of the diffraction efficiency (right scale, ○) versus the exposition of recording. The crystal thickness is 7 mm

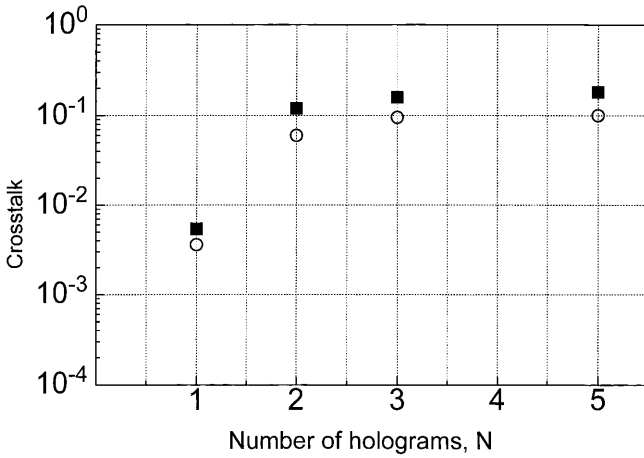


Fig. 4. The crosstalk versus of the recorded holograms number. The crystal thickness is 7 mm (○). The crystal thickness is 14 mm (■)

Using this criterion, behavior of a crosstalk in dependence of the number of recorded holograms can be investigated (Fig. 4).

3 Discussion

An excellent agreement between theory and experiment was found for EFS in the case of recording a single hologram for both hologram length in the range from -2 to $+2$ kV/cm. We also have a good agreement between theory and experiment in the case when two holograms were recorded at two different electric field values corresponding to the Rayleigh's criterion. However, it is necessary to mention two phenomena that are not described by our theoretical consideration. The first one is some discrepancy between calculated and experimental positions of the minima of the diffraction efficiency at high electric fields. One of the possible origins of this discrepancy is the piezoelectric effect [3] which results in variations in the grating spacing of the recorded hologram. The magnitude of the observed discrepancy is consistent with estimations based on the corresponding piezoelectric coefficients for LiNbO_3 . Though this phenomenon does not play a serious role in the case of a single hologram, it can be important for the analysis of crosstalk when a large number of holograms are recorded in the same crystal. The second phenomenon is a shift of the maximum diffraction efficiency to a value of the electric field different to the one at hologram recording (the effect that was mentioned in [5]). This phenomenon is associated with the photovoltaic effect which results in a charging of the crystal. We performed a detailed investigation of this effect and found

that it also depends on the nonlinearity of hologram recording at high contrast ratio of the interference pattern. We found a way to minimize this shift. A detailed description of this investigation is beyond the scope of this paper.

The experiment described above concerns the electric field selectivity. However, using (2) one can estimate the spectral selectivity in the case of using our holograms as electrically tunable spectral filters. For our set of parameters $n_e = 2.232$, $\lambda = 532.05$ nm we have a spectral selectivity of $\Delta\lambda \approx 9$ pm for a hologram thickness of $T = 7$ mm and $\Delta\lambda \approx 4.5$ pm for $T = 14$ mm. From this point of view five recorded holograms (Fig. 1c) can be considered as a five-channel electrically tunable filter with a spectral selectivity of 9 pm. This is one of the best-known selectivities for holographic filters recorded in photorefractive crystals [10–14]. Potentially, the upper limit of electrically tunable holograms can be estimated [6] to be 80 taking into account the breakdown electric field in the air of 30 kV/cm, a crystal thickness of 14 mm, and EFS of 0.75 kV/cm. Of course, this estimate depends on the certain requirements for a crosstalk. Our investigation of the crosstalk for different numbers of recorded holograms (Fig. 4) has shown that the crosstalk is almost constant when the number of recorded holograms is 5 or more. This is in a good agreement with the conception that usually it is the nearest hologram that mostly contributes to crosstalk rather than more distant holograms (see for example [6]).

Acknowledgements. Financial support of the Alexander von Humboldt Foundation (Grant IV RUS 1063840) is gratefully acknowledged.

References

1. P.J. Collier, C.B. Burckhard, L.H. Lin: *Optical Holography* (Academic Press, New York 1971)
2. M.P. Petrov, S.I. Stepanov, A.A. Kamshilin: *Ferroelectrics* **21**, 631 (1978); *Opt. Commun.* **29**, 44 (1979)
3. A. Kewitsch, M. Segev, A. Yariv, R.R. Neurgaonkar: *Opt. Lett.* **18**, 534 (1993)
4. J.V. Alvarez-Bravo, R. Muller, L. Arizmendi: *Europhys. Lett.* **31**, 443 (1995)
5. M.P. Petrov, A.V. Shamray, V.M. Petrov, J. Sanchez Mondragon: *Opt. Commun.* **153**, 305 (1998)
6. M.P. Petrov, A.V. Shamray, V.M. Petrov: *Optical Memory and Neural Networks* **7**, 19 (1998)
7. A.V. Shamray, M.P. Petrov, V.M. Petrov: In OSA TOPS Vol. 27, *Advances in Photorefractive Materials, Effects, and Devices*, 515 (Elsinore, Denmark 1999)
8. H.W. Kogelnik: *Bell Syst. Tech. J.* **48**, 2909 (1969)
9. A. Yariv: *Quantum Electronics* (Wiley, New York 1988)
10. G.A. Rakuljic, V. Leyva, A. Yariv: *Opt. Lett.* **17**, 1471 (1992)
11. S. Yin, H. Zhou, F. Zhao et al.: *Opt. Commun.* **101**, 317 (1993)
12. S. Breer, K. Buse: *Appl. Phys. B* **66**, 339 (1998)
13. J. Hurkiede, I. Nee, D. Kip, E. Krätzig: *Opt. Lett.* **23**, 1405 (1998)
14. S. Breer, H. Vogt, I. Nee, K. Buse: *Electron. Lett.* **34**, 2419 (1998)